
CONTRIBUTED PAPERS

STRUCTURE OF SHORT-AND MEDIUM-RANGE ORDER OF Fe-RICH AMORPHOUS Fe-La ALLOYS

JM. MATSUURA*, H. WAKABAYASHI**, T. GOTO***, H. KOMATSU***** and K. FUKAMICHI*****

* Miyagi National College of Technology, Nodayama Natori, Miyagi 981-12 Japan

** Tokyo Institute of Technology, Department of Applied Physics, Meguro Tokyo 152, Japan

*** Institute for Solid State Physics, The University of Tokyo, Tokyo 106, Japan

**** Department of Material Science, Faculty of Engineering, Tohoku University, Sendai 980, Japan

The ferromagnetic state of iron rich amorphous $\text{Fe}_x\text{La}_{1-x}$ alloys (a- $\text{Fe}_x\text{La}_{1-x}$) is known to become unstable with increasing iron concentration and at $x=0.9$ a cusp characteristic of a spin glass appears in AC susceptibility. In order to elucidate the correlations between the magnetic properties and the structure, we measured both large and small angle X-ray scatterings for a- $\text{Fe}_x\text{La}_{1-x}$ ($0.65 \leq x \leq 0.9$) alloys. From large angle scattering measurements, interatomic distances and partial coordination numbers between Fe-Fe, Fe-La and La-La atoms were determined. The Fe-Fe interatomic distances for these alloys are all very close to the critical value ($=2.54 \text{ \AA}$) at which an antiferromagnetic exchange competes with a ferromagnetic one. The Fe-Fe coordination number of 8.6 for a- $\text{Fe}_{0.9}\text{La}_{0.1}$ was found to be close to 8.8 for crystalline ($\text{Fe}_{0.86}\text{Al}_{0.14}$)₁₃ La alloy where the ferromagnetic ordering collapses and the antiferromagnetic one dominates. The small angle scattering for a- $\text{Fe}_{0.9}\text{La}_{0.1}$ shows pronounced high intensity in contrast to those for others ($x=0.7$ and 0.8). This fact suggests that inhomogeneous regions exist in a- $\text{Fe}_{0.9}\text{La}_{0.1}$. From the correlation function $\gamma(r)$ and Q-invariant $2\pi^2r(0)$, we conjecture that the inhomogeneous regions are consisted of iron clusters whose size is widely distributed and their volume fraction is estimated to be about 2%. The correlations of iron clusters with the spin glass state of a- $\text{Fe}_{0.9}\text{La}_{0.1}$ are discussed.

1. Introduction

Ferromagnetic state tends to be unstable and spin glass like behaviors appear when the concentration approaches to pure iron for the most of Fe-based amorphous alloys (Fukamichi et al. 1988a). For example, AC susceptibility of a- $\text{Fe}_x\text{La}_{1-x}$ alloys ($0.7 \leq x \leq 0.875$) at the low field ($H=1.0 \text{ Oe}$) shows that the Curie temperature, T_c , decreases from 287 K to 230 K with increasing Fe concentration (Wakabayashi 1988). An alloy in this concentration region exhibits transition from a ferromagnetic to a spin glass state at a freezing temperature T_f ($< T_c$) below which AC susceptibility falls down. Furthermore, AC susceptibility of a- $\text{Fe}_x\text{La}_{1-x}$ alloys with $x>0.9$ shows a cusp typical of a spin glass. Besides a-FeR alloys, other Fe rich amorphous alloys like as Fe-B (Fukamichi 1983) and Fe-Zr (Saito et al. 1986) are known that the ferromagnetic state becomes unstable with the Fe concentration approaching to pure iron. The reason why the ferromagnetic state of Fe-based amorphous alloys becomes unstable with their concentration ap-

proaching to pure iron has been discussed in connection with fcc $\gamma\text{-Fe}$; since a short range structure of an amorphous pure metal which can be well represented by the dense random packing of hard spheres is similar to fcc one, amorphous pure iron should have antiferromagnetic couplings like as fcc $\gamma\text{-Fe}$. However, the values of Fe-Fe interatomic distance of an amorphous alloy is not unique but distributed, the coexistence of ferro- and antiferro-couplings are likely to occur. Furthermore, the concentration region where ferromagnetic instability takes place is close to the critical concentration of amorphization for Fe-based alloys (Fukamichi and Hiroyoshi 1985). Therefore, structural or compositional inhomogeneity is likely to occur and this also affects the occurrence of ferromagnetic instability of Fe-rich amorphous alloys. Few works have been done, however, on the correlations between structural or compositional inhomogeneity and the ferromagnetic instability of Fe-rich amorphous alloys.

In order to elucidate how the structural changes are associated with the occurrence of the spin glass like behavior for a-Fe_{0.9}La_{0.1} and with the ferromagnetic instability of a-Fe_xLa_{1-x} (0.65 ≤ x ≤ 0.9) alloys, we have measured large angle (LAXS) and small angle X-ray scatterings (SAXS). Because LAXS provides structural information on the short range order whereas SAXS on the medium range order, it is advantageous to utilize both methods for the structural studies of amorphous alloys. Furthermore, as discussed in the previous work (Matsuura et al. 1988a and Matsuura et al. 1988b) amorphous Fe-La alloys are fairly convenient substances for the study of the structure by X-ray diffraction because the atomic radius of La (1.88 Å) is the largest among rare earth metals; the ratio of the Goldschmidt radius of La to that of Fe amounts to 1.44. Moreover, X-ray atomic form factor of La atom is so large that the weighting factors for La-La and La Fe correlations are considerably large even in a Fe-rich concentration region (see Table 1). Therefore, their partial distribution functions can be easily distinguished and deduced from a total radial distribution function without any troublesome experiments.

2. Experimental Procedures and Data Analysis

All of the samples used for X-ray diffraction were prepared by high rate DC sputtering, the condition of which were as follows; the target voltage and current were 1.0 kV and 60 mA, respectively and the Ar gas pressure was 5.3 Pa. The samples were deposited onto a water-cooled Cu substrate for LAXS measurements and onto Al foil (0.015 mm thick) for SAXS ones. The sample thickness was about 0.4mm for LAXS and 0.02-0.03 mm for SAXS. MoKα was used as X-ray source. A curved quartz crystal and a zirconium filter were used for the monochromator in the measurements of LAXS and SAXS, respectively. Since the details of the measurements and the data analysis for LAXS were described previously (Matsuura 1988b), a brief description about the SAXS measurements will be given below.

The Kratky camera, Rigaku 2203E, was used for the SAXS measurements. The widths of incident and receiving slits were 0.04 and 0.08mm, respectively. The height of a longitudinal slit was 10 mm. In order to remove effects of primary beam and parasitic scattering, background intensity, P_b(Q), was measured by displacing a sample from the ordinary position at the middle of the U-slits from which sample scattering

does not reach a counter. Corrected intensity P_c(Q) was obtained by subtracting P_b(Q) from P_s(Q):

$$P_c(Q) = P_s(Q) - P_b(Q) \quad (1)$$

The slit length correction assuming the infinite slit length was carried out by the method given by Guinier and Fournet (1955), and Schmidt (1976), i.e.

$$I(Q) = \frac{2}{\lambda W_l(0)} \int_0^\infty \frac{P' \sqrt{Q^2 + u^2}}{\sqrt{Q^2 + u^2}} du \quad (2)$$

where Q is the wave number (Å⁻¹), given as Q = (4π/λ)sinθ (θ is the scattering angle), λ the wave length, W_l(0) the slit-length weighting factor and P'(x) ≡ dP(x)/dx. The absolute scattering intensity, J(Q), can be determined from the scattering intensity I(Q), i.e.

$$J(Q) = K_0 I(Q) \quad (3)$$

and

$$K_0 = K / \{ \gamma_T^2 N_v (t e^{-\mu t}) \} \quad (4)$$

where γ_T is the Thomson radius, N, the scattering units per unit volume in the sample thickness t, μ the mass absorption coefficient and K the characteristic constant of the Kratky camera given by

$$K = \frac{\kappa_{poly}(Q') (e^{-\mu t})_{poly} W_l(0)}{P_{poly}(Q')} \quad (5)$$

where κ_{poly} is the characteristic value of the Lupolen used in the present work (=0.0365 for CuKα) and P_{poly}(Q') the observed intensity of the Lupolen at Q' (=0.042 Å⁻¹) in the same condition as the sample measurement.

The correlation function γ(r) and the Q-invariant 2π²γ(0) defined by the following equations (6) and (7), respectively, are estimated from the absolute scattering intensity J(Q).

$$\gamma(r) = \frac{1}{2\pi^2 r} \int_0^\infty Q J(Q) \sin(Qr) dQ \quad (6)$$

$$\gamma(0) = \frac{1}{2\pi^2} \int_0^\infty Q^2 J(Q) dQ \quad (7)$$

The Q-invariant (=2π²γ(0)) is related with electron density fluctuation Δρ (= ρ - ρ₀) and volume fraction V_f of particles, i.e.

$$\gamma(0) = \Delta\rho^2 V_f (1 - V_f) \quad (8)$$

where ρ and ρ₀ are electron densities of particles and matrix, respectively.

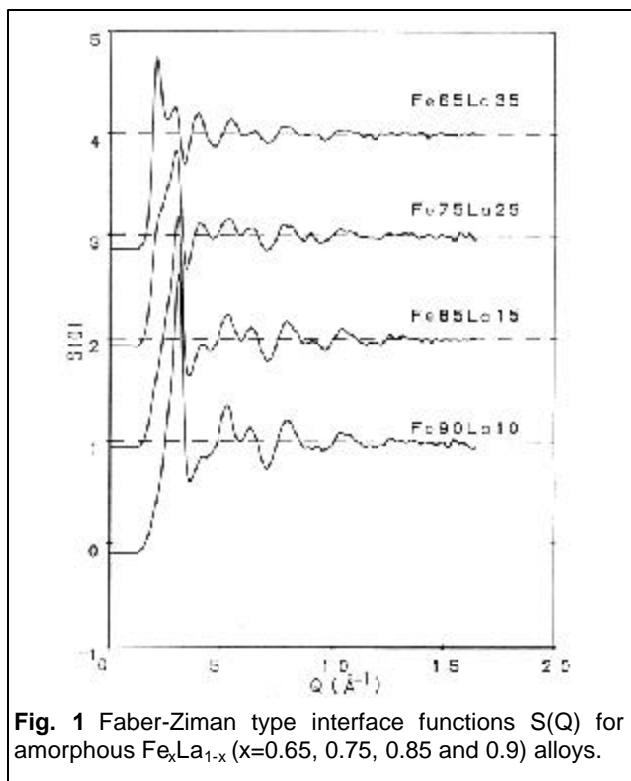


Fig. 1 Faber-Ziman type interface functions $S(Q)$ for amorphous $\text{Fe}_x\text{La}_{1-x}$ ($x=0.65, 0.75, 0.85$ and 0.9) alloys.

Table 1 X-ray weighting factors $w_{ij}/\langle f^2 \rangle$ for distribution functions of $\text{Fe}_x\text{La}_{1-x}$ alloys.

	$\text{Fe}_{0.9}\text{La}_{0.1}$	$\text{Fe}_{0.85}\text{La}_{0.15}$	$\text{Fe}_{0.75}\text{La}_{0.25}$	$\text{Fe}_{0.65}\text{La}_{0.35}$
$w_{\text{Fe-Fe}}$	0.65	0.52	0.33	0.21
$2w_{\text{Fe-La}}$	0.31	0.40	0.48	0.50
$w_{\text{La-La}}$	0.04	0.08	0.18	0.29

3. Results

3.1 Large Angle X-ray Scattering

Fig. 1 shows the Faber-Ziman type interference functions $S(Q)$ for a- $\text{Fe}_x\text{La}_{1-x}$ ($x=0.65, 0.75, 0.85$ and 0.9) alloys. Because of the large X-ray atomic form factor of La atom, the weighting factor of the partial interference function between La atoms, $w_{\text{La-La}}$, increases rapidly with La concentration as shown in Table 1. The intensity of the La-La interference, therefore, exceeds the Fe-Fe one with increasing La concentration and the first peak splits into a double peak at 35 at.% La.

The reduced radial distribution function $G(r)$, which is defined as

$$G(r) = 4\pi r(g(r) - g_0) \quad (9)$$

where $g(r)$ is the atomic distribution function and g_0 the mean number density. And it is derived by the Fourier transformation of $S(Q)$, i.e.

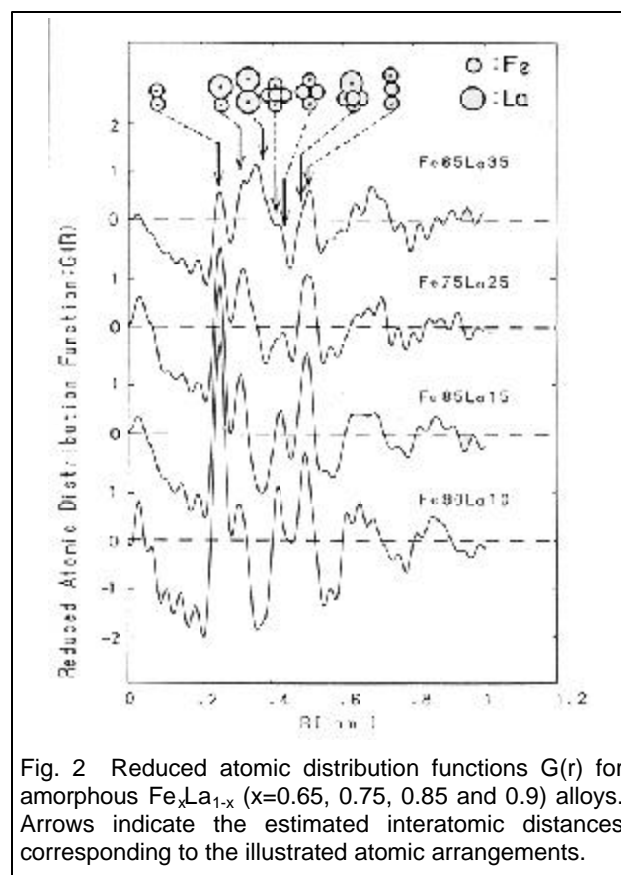


Fig. 2 Reduced atomic distribution functions $G(r)$ for amorphous $\text{Fe}_x\text{La}_{1-x}$ ($x=0.65, 0.75, 0.85$ and 0.9) alloys. Arrows indicate the estimated interatomic distances corresponding to the illustrated atomic arrangements.

$$G(r) = \frac{2}{\pi} \int_0^{\infty} Q[S(Q) - 1] \sin(Qr) dQ \quad (10)$$

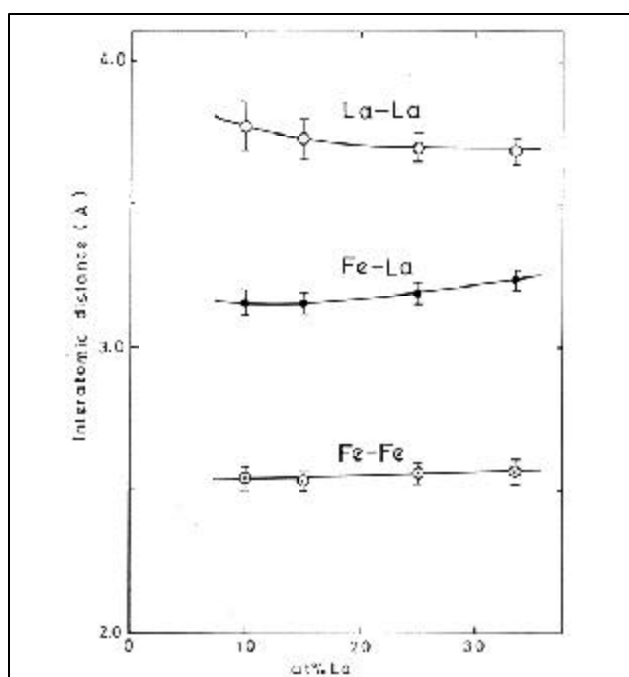
The g_0 values are referred from the previous work (Matsuura et al. 1988b). Resultant $G(r)$ curves are shown in Fig. 2. Since the ratio of the atomic radius between Fe and La, $r_{\text{La}}/r_{\text{Fe}}$, is relatively large, the first three peaks, i.e. Fe-Fe, Fe-La and La-La correlations, are clearly distinctive and even the second neighbors can be identified as shown in Fig. 2. The arrows show the estimated interatomic distances of the respective atomic arrangements illustrated in the same figure. The Goldschmidt atomic radii were used in these estimations. The interatomic distances and partial coordination numbers were determined by fitting the experimental $G(r)$ curves to those of sum of Gaussian functions. The results of the concentration dependences of the interatomic distances and the partial coordination numbers between Fe-Fe, Fe-La and La-La are illustrated in Figs. 3 and 4, respectively and also listed in Table 2. The normalized order parameter η^0 defined by Cargill and Spaepen (1981) are estimated from the partial coordination numbers and listed in Table 2 and plotted in Fig. 5. Table 2 also includes full width of the half maximum (FWHM) of the three

Table 2 Structural parameters determined from X-ray diffraction of a-Fe_xLa_{1-x} alloys.

Fe _x La _{1-x}	Interatomic distance (Å)						Coordination number			Order parameter		FWHM** of 1st nearest neighbor peak in G(r) (Å)		
	1st Nearest Neighbor			2nd Nearest Neighbor			Fe-Fe	Fe-La	La-La	η	η ⁰	Fe-Fe	Fe-La	La-La
	Fe-Fe	Fe-La	La-La	4th	5th	6th	Fe-Fe	Fe-La	La-La					
0.95	2.542	3.161	3.774	4.143	4.516	4.982	8.55	2.24	3.47	0.061	0.250	0.37	0.62	0.31
0.85	2.536	3.161	3.731	4.189	4.584	5.001	7.78	2.72	4.10	0.049	0.149	0.35	0.60	0.42
0.75	2.566	3.193	3.702	4.059	4.387	4.954	6.92	3.51	5.19	0.064	0.013	0.34	0.63	0.55
0.67	2.571	3.240	3.696	4.243	*	4/908	6.27	3.51	5.62	-0.085	-0.132	0.37	0.52	0.43
0.65	2.545	3.168	3.624	3.923	4.246	4.869	6.28	3.00	6.20	-0.204	-0.299	0.36	0.53	0.47

* Cannot be distinguished. ** FWHM: Full width at half maximum.

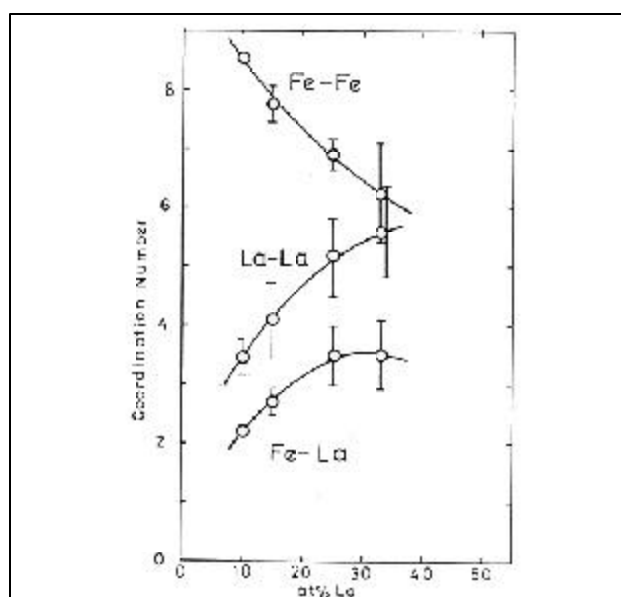
cf η, order parameter and η⁰, normalized order parameter defined by Cargill and Spaepen (1981).

**Fig. 3** Concentration dependences of the interatomic distances of the first Fe-Fe, Fe-La and La-La neighbors of amorphous Fe_xLa_{1-x} alloys.

nearest neighbor correlation peaks in the G(r) curve. The present values in Table 2 are a little different from the previous ones (Matsuura et al. 1988b) because of an improvement of data analysis; an elimination of inelastic scattering contribution due to utilizing a monochromator is taken into account in the present work.

3.2 Small Angle X-ray Scattering

Plots of logP_c(Q) vs. log Q for a-Fe_xLa_{1-x} (x=0.7, 0.8 and 0.9) alloys are shown in Fig. 6. The small angle scattering intensity for the alloy with x=0.9 is

**Fig. 4** Partial coordination numbers of the first Fe-Fe, Fe-La and La-La neighbors against La concentration of amorphous Fe_xLa_{1-x} alloys.

extremely larger than those with x=0.8 and 0.7 by more than two orders of magnitude. Fig. 6 indicates that there are two regions where the P_c(Q) is represented as a different power of Q for a-Fe_{0.9}La_{0.1}. Logarithm of the absolute intensity, logJ(Q), versus Q², i.e. Guinier plot, are plotted in Fig. 7 for a-Fe_{0.9}La_{0.1}. This result indicates that a unique radius of gyration for a-Fe_{0.9}La_{0.1} alloy can not be determined, which may suggest a wide distribution of the particle size. The correlation function γ(r) for a-Fe_{0.9}La_{0.1} was deduced from the absolute scattering intensity J(Q) using Eq. (6) and shown in Fig. 8. Though a definite correlation length can not be defined from the γ(r) curve like as the Guinier plot,

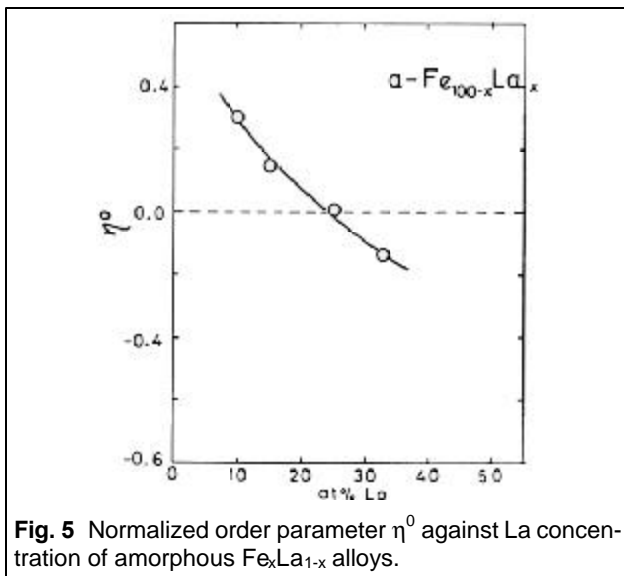


Fig. 5 Normalized order parameter η^0 against La concentration of amorphous $\text{Fe}_x\text{La}_{1-x}$ alloys.

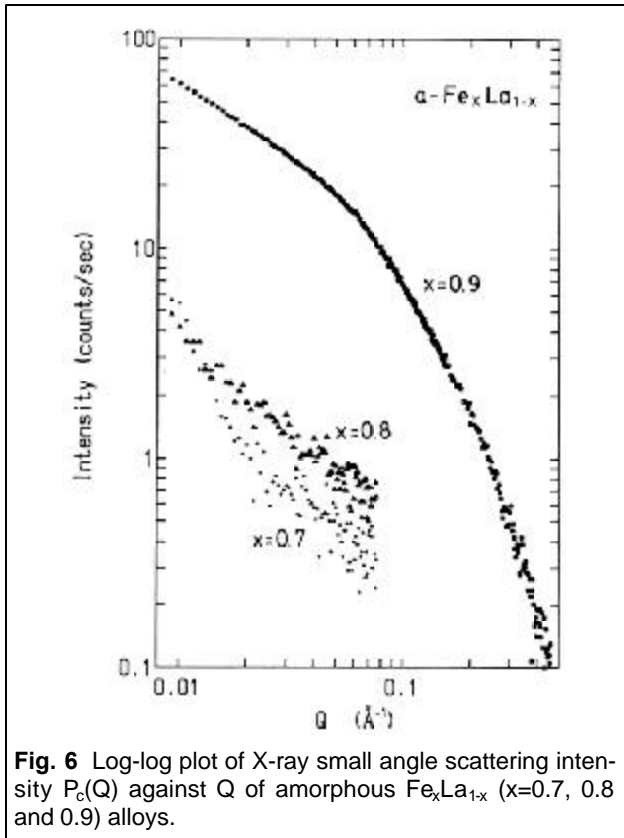


Fig. 6 Log-log plot of X-ray small angle scattering intensity $P_c(Q)$ against Q of amorphous $\text{Fe}_x\text{La}_{1-x}$ ($x=0.7, 0.8$ and 0.9) alloys.

the correlation length ranges from 40 to 120 Å. The $\chi(0)$ value estimated from the absolute intensity $J(Q)$ using Eq. (7) leads to 0.24×10^{46} (eu \cdot cm $^{-6}$) for a- $\text{Fe}_{0.9}\text{La}_{0.1}$.

4. Discussion

As described before the ferromagnetic state of a- $\text{Fe}_x\text{La}_{1-x}$ alloys becomes unstable with increasing Fe concentration, and finally at 90 at.% Fe the AC sus-

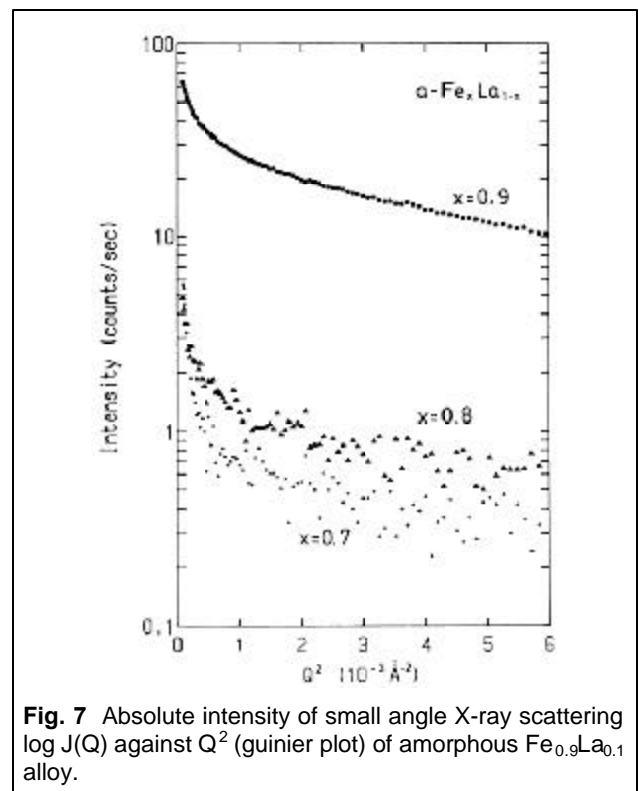


Fig. 7 Absolute intensity of small angle X-ray scattering $\log J(Q)$ against Q^2 (guinier plot) of amorphous $\text{Fe}_{0.9}\text{La}_{0.1}$ alloy.

ceptibility in a weak field shows a cusp typical of a spin glass state. The interatomic distances between Fe-Fe and Fe-La atoms are shortened slightly with increasing Fe concentration, while that of La-La atoms is elongated as shown in Fig. 3. The Fe-Fe interatomic distance of γ -Fe precipitated in Cu is 2.529 Å at 70K (Gonser et al. 1963) and the critical Fe-Fe interatomic distance at which an antiferromagnetic coupling competes with ferromagnetic one has been estimated as 2.54 Å (Forrester et al. 1979). The alloys of a- $\text{Fe}_x\text{La}_{1-x}$ ($0.65 \leq x \leq 0.9$) have the Fe-Fe interatomic distances close to the critical value as shown in Table 2. Therefore, ferromagnetic states of a- $\text{Fe}_{0.9}\text{La}_{0.1}$ are inclined to be unstable. Another important effect of the Fe-Fe interatomic distance on the ferromagnetic instability is a distance fluctuation around the mean value, i.e. $\sqrt{(\delta r)^2}/r$, where r is the position of Fe-Fe 1st neighbor peak in $G(r)$. The greater the fluctuation is, the more unstable a ferromagnetic state becomes (Kakehashi 1988). We can see from Table 2 that the FWHM of the 1st Fe-Fe neighbor peak in $G(r)$ increases with increasing Fe concentration for those alloys with $x=0.75 \sim 0.9$.

The magnetic state of Fe-rich a- $\text{Fe}_x\text{La}_{1-x}$ must be affected not only by the Fe-Fe interatomic distance but also by the Fe-Fe coordination. The three partial coordination numbers of Fe-Fe, Fe-La and La-La

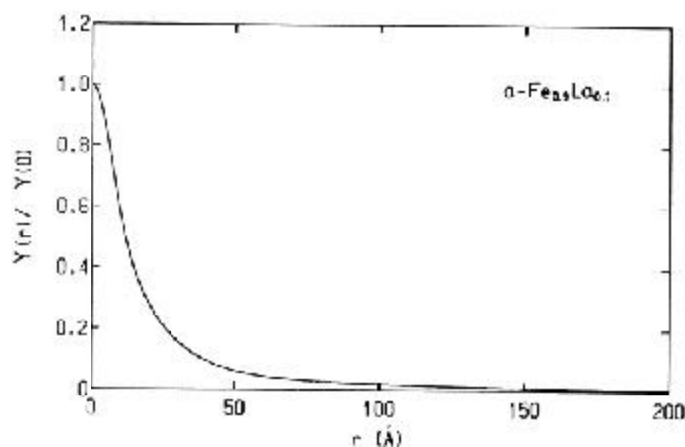


Fig. 8 Correlation function $\gamma(r)$ of amorphous $\text{Fe}_{0.9}\text{La}_{0.1}$ alloy.

pairs vary monotonically with the Fe concentration. The present results indicate that the magnetic properties of $a\text{-Fe}_x\text{La}_{1-x}$ are strongly correlated with the Fe-Fe coordination as will be described below.

It seems instructive to compare the magnetic properties of $a\text{-Fe}_{0.9}\text{La}_{0.1}$ alloy with those of crystalline $(\text{Fe}_x\text{Al}_{1-x})_{13}\text{La}$ alloys. Crystalline $(\text{Fe}_x\text{Al}_{1-x})_{13}\text{La}$ alloys exhibit three different magnetic states depending on the iron concentration: (1) a micro magnetic state ($0.46 \leq x < 0.62$), (2) a soft ferromagnetic state ($0.62 < x \leq 0.86$) and (3) an antiferromagnetic state ($0.86 < x \leq 0.92$) (Palstra et al. 1985). There are two different iron sites in the $(\text{Fe}_x\text{Al}_{1-x})_{13}\text{La}$ alloys i.e. FeI and FeII. Both sites have high coordination number, 12 and 10 for FeI and FeII, respectively. With increasing iron concentration, the mean Fe-Fe coordination number increases up to 10.2 for the $x = 1$. Under such a high coordination, the ferromagnetic ordering collapses and an antiferromagnetic state appears like as $\gamma\text{-Fe}$. It is very interesting to denote that the ferromagnetic state of $c\text{-}(\text{Fe}_x\text{Al}_{1-x})_{13}\text{La}$ alloys transforms into the antiferromagnetic one at the Fe-Fe coordination of 8.8 which is close to the present value of 8.6 where $a\text{-Fe}_x\text{La}_{1-x}$ alloy exhibits a cusp typical of a spin glass in AC susceptibility. Therefore, the Fe-Fe coordination number 8.6 ~ 8.8 may be the critical value below which ferromagnetic long range order is stable and above which an antiferromagnetic coupling should prevail. Though ferromagnetic states for both alloys turn out to be unstable with increasing iron concentration toward pure iron, neither an anti-ferromagnetic long range order nor a sharp spin flip occurs in $a\text{-Fe}_{0.9}\text{La}_{0.1}$ unlike $c\text{-}(\text{Fe}_x\text{Al}_{1-x})_{13}\text{La}$. These differences can be ascribed mainly to the disordered structure of $a\text{-Fe}_x\text{La}_{1-x}$ alloys because a long range antiferromag-

netic structure can not be established in the disordered structure such as amorphous alloys exhibiting a spin frustration (Kaneyoshi 1983). Furthermore, the Fe-Fe interatomic distance for $a\text{-Fe}_{0.9}\text{La}_{0.1}$ ($=2.542\text{\AA}$) is not so short as that for $c\text{-}(\text{Fe}_x\text{Al}_{1-x})_{13}\text{La}$ ($=2.445\text{\AA}$ for $x = 0.86$). Therefore an antiferromagnetic coupling for $a\text{-Fe}_{0.9}\text{La}_{0.1}$ should be weaker than $c\text{-}(\text{Fe}_x\text{Al}_{1-x})_{13}\text{La}$.

We can reasonably inspect that the considerably high intensity of the small angle scattering correlates with the spin glass like behavior for $a\text{-Fe}_{0.9}\text{La}_{0.1}$. Since SAXS reflects a structure of medium range order, the fairly large SAXS intensity found in $a\text{-Fe}_{0.9}\text{La}_{0.1}$ alloy suggests that there are some regions inhomogeneous with electron density. The size of the regions can be estimated to be 40 - 120 \AA from the $\gamma(r)$ curve. Three cases are probable which cause such an electron density fluctuation; the existence of (1) iron rich region, (2) La rich region and (3) their mixture. The third case is out of numerical treatment. As an extreme case if the $a\text{-Fe}_{0.9}\text{La}_{0.1}$ were to be phase-separated into two pure elements, the $\gamma(0)$ value could be easily estimated assuming each phase had the same electron density as the crystalline one i.e. bcc Fe or hcp La. The calculated $\eta\gamma(0)$ value ($25 \times 10^{46} \text{ eu} \cdot \text{cm}^{-6}$) is about one hundred times greater than the experimental one. Furthermore, the results of the order parameters η^0 shown in Fig. 5 suggest that the structure of $a\text{-Fe}_{0.9}\text{La}_{0.1}$ exhibits chemical preference for Fe-La neighbors rather than clustering. Therefore, it is implausible that lanthanum atoms in $a\text{-Fe}_{0.9}\text{La}_{0.1}$ would be concentrated into clusters. Alternatively, the most part of matrix is assumed to be homogeneous and only a small number of iron atoms clusters, whose short range structure must be similar to that of

fcc γ -Fe. In this case the average electron density ρ_a and density fluctuation $\Delta\rho$ can be denoted as

$$\rho_a = V_f \rho_{\gamma\text{-Fe}} + (1 - V_f) \rho_0 \quad (11)$$

and

$$\Delta\rho = \rho_{\gamma\text{-Fe}} - \rho_0 \quad (12)$$

where $\rho_{\gamma\text{-Fe}}$ and V_f are the electron density of the γ -Fe like particles and their volume fraction, respectively, and ρ_0 the electron density in the homogeneous part. The volume fraction V_f can be evaluated from Eqs. (8), (11) and (12), and the $\gamma_{\text{exp}}(0)$, i.e.

$$V_f = \frac{\gamma_{\text{exp}}(0)}{(\rho_a - \rho_{\gamma\text{-Fe}})^2 + \gamma_{\text{exp}}(0)} \quad (13)$$

The electron density of γ -Fe, $\rho_{\gamma\text{-Fe}}$ is estimated by extrapolating the lattice constant (Pearson 1958) down to the room temperature (20°C) and ρ_a , from the density measurement i.e. $\rho_{\gamma\text{-Fe}} = 2.31 \times 10^{48}$ (eu · cm⁻³) and $\rho_a = 1.95 \times 10^{48}$ (eu · cm⁻³). The resultant V_f value is 0.019, namely about 2% of the total volume. Therefore, we can conjecture that a-Fe_{0.9}La_{0.1} alloy contains Fe-concentrated regions, 40-120 Å in size and about 2% in volume, where an antiferromagnetic coupling dominates because of the high Fe Fe coordination and the spin frustration due to a topological constriction (Kaneyoshi 1983).

Since the composition of a-Fe_{0.9}La_{0.1} is close to the critical concentration region where amorphous state can be formed by sputtering, a structural or a compositional fluctuation is likely to occur. Therefore, iron clusters is apt to be formed in a concentration region near pure iron. These iron clusters in a Fe_{0.9}La_{0.1} must affect the magnetic state of the surrounding matrix through their boundaries. The ferromagnetic state of the matrix itself is unstable because the Fe-Fe coordination is relatively large and the Fe-Fe interatomic distance is close to the critical value of 2.54 Å. Therefore, the iron clusters where antiferromagnetic couplings prevail against ferromagnetic ones work to enhance the ferromagnetic instability and lead to the appearance of the spin glass state of a-Fe_{0.9}La_{0.1}.

5. Summary

The results of large angle X-ray scattering for a-Fe_xLa_{1-x} alloys indicate the followings; (1) the Fe-Fe interatomic distances are close to the critical value of a competition between ferro and antiferromagnetic exchanges (2) the Fe-Fe coordination number in-

creases with Fe concentration and attains up to 8.55 for x=0.9 and (3) the fluctuation of the Fe-Fe interatomic distance is largest for the alloy with x=0.9. These facts suggest that an antiferromagnetic coupling prevails against ferromagnetic one with increasing Fe concentration and finally a spin glass state appears at x=0.9.

The results of small angle X-ray scattering for a-Fe_xLa_{1-x} show that there are inhomogeneous regions consisted probably of iron clusters in a-Fe_{0.9}La_{0.1} but not in other alloys. This implies that iron clusters in a-Fe_{0.9}La_{0.1} are associated with the spin glass behavior of this alloy; iron clusters can enhance the instability of ferromagnetic couplings in the matrix.

References (alphabetical order)

- Cargill, III, G. S. and Speapen, F.: J. Non-Cry. Solids, **43**, (198 1), 91 95.
- Forrester, D. W. Koon, N.C. Schelleng, J. H. and Rhyne, J. J.: J. Appl. Phys., **50**, (1979), 7336-41.
- Fukamichi, K.: *Amorphous Metallic Glasses*, ed. by Luborsky, F. E., Butterworths, London, 1983, pp. 318-40.
- Fukamichi, K. and Hiroyoshi, H.: Sci. Rep. RITU, **A32** (1985), 154-67.
- Fukamichi, K., Komatsu, H., Goto, T. and Wakabayashi, H.: Physics, **B149** (1988a), 276-80.
- Fukamichi, K., Komatsu, H. Goto, T., Wakabayashi, H. and Matsuura, M.: MRS Int. Meeting, 1988, Tokyo, 1988b, in press. Gonser, U., Meechan, C. J., Muir, A. H. and Wiedersich, H.: J. Appl. Phys., **24** (1963), 2373-8.
- Guinier, A. and Fournet, G.: *Small Angle Scattering of X-ray*, John Wiley and Sons, Inc., New York, 1955, pp. 111-20.
- Kakehashi, Y.: private communication, 1988.
- Kaneyoshi, T., *Glassy Metals*, ed. by Hasegawa, R., CRC Press Inc., Florida 1983, pp. 37-64.
- Matsuura, M., Fukunaga, T., Fukamichi, K., Sato, Y. and Suzuki, K.: Zeitschrift für Physikalische Chemie Neue Folge, **157** (1988a), 85-89.
- Matsuura, M., Fukunaga, T., Fukamichi, K. and Suzuki, K.: Solid State Commu., **66**, (1988b), 333 7.
- Palstra, T. T. M., Nieuwenhuys, G. J. Mydosh, J. A. and Buschow, K. H. J.: Phys. Rev., **B31** (1985), 4622-32.
- Pearson, W. B., *A Handbook of Lattice Spacings and Structures of Metals and Alloys*, 1958, p. 625.
- Saito, N., Hiroyoshi, H., Fukamichi, K. and Nakagawa, Y.: J. Phys., **F16** (1986), 911-9.
- Schmidt, P. W.: *Crystallographic Computing Techniques*, ed. by Ahmed, F. R., Huml, K., Sedlacek, B., Munksgaard, Copenhagen, 1976, pp. 363-375.
- Wakabayashi, H.: Doctor Thesis of Tokyo Institute of Technology, Department of Applied Physics, Meguro Tokyo, Japan, 1988.

(This paper was originally contributed to J. Physics F.)